

# Lifetime measurements ( $T_1$ ) of electron spins in Si/SiGe quantum dots

Robert R. Hayes,\* Andrey A. Kiselev, Matthew G. Borselli, Steven S. Bui,  
Edward T. Croke III, Peter W. Deelman, Brett M. Maune, Ivan Milosavljevic, Jeong-Sun  
Moon, Richard S. Ross, Adele E. Schmitz, Mark F. Gyure, and Andrew T. Hunter  
*HRL Laboratories, LLC, Malibu, CA 90265, USA*  
(Dated: February 3, 2022)

We have observed the Zeeman-split excited state of a spin- $1/2$  multi-electron Si/SiGe depletion quantum dot and measured its spin relaxation time  $T_1$  in magnetic fields up to 2 T. Using a new step-and-reach technique, we have experimentally verified the  $g$ -value of  $2.0 \pm 0.1$  for the observed Zeeman doublet. We have also measured  $T_1$  of single- and multi-electron spins in InGaAs quantum dots. The lifetimes of the Si/SiGe system are appreciably longer than those for InGaAs dots for comparable magnetic field strengths, but both approach one second at sufficiently low fields ( $< 1$  T for Si, and  $< 0.2$  T for InGaAs).

**Introduction** Gate-defined quantum dots (QD) in the Si/SiGe material system have been touted as one of the more promising candidates for spin-based quantum computation, primarily because of the long decoherence time  $T_2$  expected for electron spins in Si [1]. Because  $T_1$  establishes a natural upper bound on  $T_2$ , a measurement of the spin relaxation time  $T_1$  for isolated electrons in any Si-based system has been an important and actively-pursued objective [2, 3]. Although there has been significant progress in fabricating and testing few-electron Si/SiGe dots [3], there has been, up until now, no direct measurement showing the anticipated long spin-relaxation lifetimes. Indeed, there has been no direct measurement of a Zeeman splitting for either single- or few-electron states in any Si-based quantum dot.

In this Letter, we report the first direct experimental confirmation of a Zeeman spin excited state in a few-electron Si/SiGe quantum dot, and a measurement of its lifetime as a function of magnetic field. We also report comparable data for InGaAs dots, used as a testbed for our measurement techniques. These dots could be emptied, thus allowing us to measure single-electron spins.

**Dot Particulars** Figure 1 shows the electrode layout and epitaxial structure for our Si/Si<sub>0.7</sub>Ge<sub>0.3</sub> dot. The InGaAs/InAlAs/InP depletion dot had an almost identical electrode geometry, but a different epitaxial structure which incorporated two quantum wells, not one, so that the wafer could also be used for accumulation-mode devices (described elsewhere [4]). In our depletion-mode devices, the upper well in the InGaAs structure played no role.

**Measurement** The dot was electrostatically formed using conventional techniques [5]. We found, empirically, that the lowest number of electrons on the dot,  $N_{\min}$ , can be reached when the T-R channel is pinched off and the T-B channel kept open. However, as the electrode voltages are lowered to drive additional

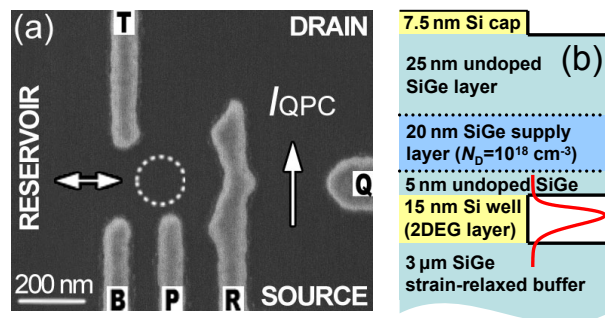


Figure 1: (a) A SEM image of the metal electrodes on the device surface. The dashed circle is the estimated location of the charge disc formed by the dot electrons. The arrow shows the tunneling channel used in all measurements. (b) The CVD-grown Si/Si<sub>0.7</sub>Ge<sub>0.3</sub> heterostructure with a 2DEG mobility of 10 000-15 000 cm<sup>2</sup>/Vs and a charge density of  $4.6\text{-}5.3 \times 10^{11}$  cm<sup>-2</sup> (both measured at 4.2 K).

electrons off the dot, the T-B channel eventually becomes pinched off also, preventing any further reduction in  $N$ . Although we routinely reached  $N = 0$  in InGaAs dots before this happened, the lowest value of  $N$  obtained for Si/SiGe dots was likely 7, and this only after several painstaking redesigns of the electrodes in which the gaps for the T-B and T-R channels were progressively widened.

When  $N_{\min}$  was reached,  $T_1$  was measured by repeatedly applying a three-step bias sequence to one of the electrodes (a technique first used in [6]). The response of the charge-monitoring current,  $I_{\text{QPC}}$ , to the bias changes is twofold: (i) a drop in the current by a fixed amount when an electron is (spontaneously) added to the dot, and an increase when it is removed, as shown by the dashed lines in Figure 2, and (ii) a replication of the bias sequence due to unwanted capacitive coupling of the driven electrode to the R-Q channel.

The key response is the rectangular pulse formed

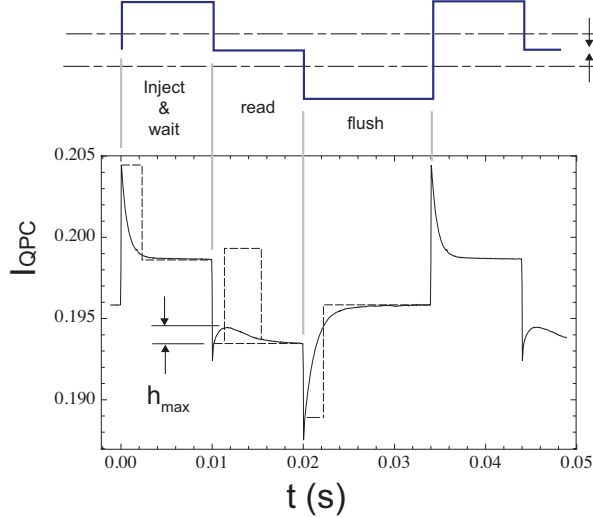


Figure 2: The Delft three-step sequence used for the  $T_1$  measurement [6]. The first step loads an electron into the excited state with probability  $p_0$ , or into the ground state with probability  $(1 - p_0)$ , and then waits. If the electron is in the excited state, and survives the wait-time without decaying to the ground state, the second step removes it from the dot and reloads another from the reservoir into the ground state. The third step flushes the ground state electron off the dot, so that the cycle can be repeated. The dashed lines are an artistic rendition of instantaneous values of  $I_{QPC}$  that occur during a typical cycle, the solid curve is an actual time-average of 10 000 of these events.

during the read interval, which only forms when a loaded excited-state electron does *not* decay to the ground state during the wait-time. A time-average of this rectangular pulse gives a “spin bump” having the analytic form

$$h(t) \propto p(e^{-t/\tau_1} - e^{-t/\tau_2})/(\tau_2/\tau_1 - 1)$$

where  $\tau_1$  ( $\tau_2$ ) is the tunneling time off of (onto) the dot, and  $p$  is the fraction of electrons that load into the excited state during the inject pulse and survive the wait-time without decaying to the ground state. For equal tunneling times this expression reduces to  $h(t) \propto p(t/\tau) e^{-t/\tau}$ .

With increasing wait-time  $t_{\text{wait}}$ , the fraction of instances when an unload-reload pulse is formed during the read interval will decay exponentially as  $p = p_0 e^{-t_{\text{wait}}/T_1}$  (assuming that the characteristic time  $T_1 \gg \tau$ ). The spin bump height  $h_{\text{max}}$ , plotted versus  $t_{\text{wait}}$ , will show the same exponential decay, as demonstrated by the data in Fig. 3.

There are two advantages of using time-averaging rather than the pulse-counting of [6]: (i) the high signal-to-noise ratio required to reliably detect individual pulses is not needed, and (ii) the false counts

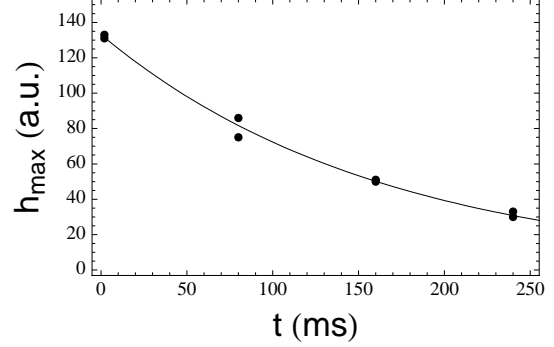


Figure 3: Spin bump height versus wait-time for our Si/SiGe dot in a magnetic field of 1.5 T. The solid curve, an exponential fit to the data (circles), gives a  $T_1$  of 164 ms.

due to random telegraph signals (RTS) that will unavoidably occur when the read level is near the lower Zeeman level contribute trivially, because the average of RTS-induced pulses is a straight line. What is lost by using the averaging approach is a direct measure of the branching ratio,  $p_0$ . However,  $p_0$  is not needed for a determination of  $T_1$ .

**Zeeman splitting** The spin-bump appears when, and only when, the amplitude of the inject-and-wait pulse is sufficient to reach the first excited state. This suggests a step-and-reach technique for measuring the Zeeman splitting. One places the read level a known amount above the ground state (the *step* process), and then progressively *reaches* up with the inject pulse until a bump appears. The exact point of appearance of the bump is determined experimentally by measuring the bump height for several values of step-plus-reach amplitude just beyond the first appearance of the bump, and then extrapolating backward to determine the zero-intercept. To convert the combined step and reach amplitudes to an actual energy, we used a temperature sweep and the known relation between the width of a Coulomb Blockade peak and the dot’s temperature [7] to determine both the lever arm,  $\alpha$ , and the effective base temperature of the system, 12.55 V<sub>Plunger</sub>/eV and 48 mK, respectively.

The Zeeman splitting was measured for several values of the magnetic field using this technique. Two sets of measurements were made, one with the magnetic field increasing with each successive point, the other with it decreasing, in order to look for hysteretic effects (which we did not see). These data are plotted in Fig. 4. One sees immediately that there is a small but non-negligible deviation from a straight line at higher values of  $B$ , which we suspect may be caused by a small component of the magnetic field normal to the 2DEG. We have fit the 9 measured points to the somewhat arbitrary function  $E_Z = a + bB + cB^n$ , using

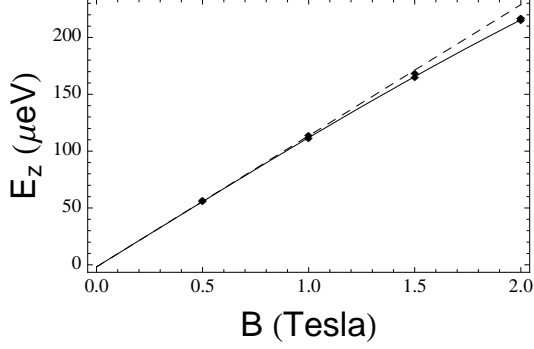


Figure 4: The Zeeman splitting as a function of magnetic field. The solid curve is a fit with  $E_z = a + bB + cB^3$ , the dashed curve is the linear portion of that expression.

values of  $n$  ranging from 2 to infinity, and have found that these fits give a zero-field value of  $g$  that ranges from 2.1 to 1.9. Although the  $g$ -value that results from the fit having the lowest variance and proper symmetry ( $n = 3$ ) is 1.99, all fits appear equally acceptable to the eye, making it difficult to choose one over another. Our estimate of  $g$  is thus  $2.0 \pm 0.1$ , in agreement with theoretical expectations and measurements on impurity-bound electrons in Si [8].

**Multi-electron dots** Our measurements of  $T_1$  for Si/SiGe are for an  $N$ -electron dot that we believe had 7 electrons (5 to 7 electrons if based exclusively on the energy spacings between Coulomb Blockade peaks, or, more definitively, 7 electrons when further constrained by the filling sequence of spin states as discussed below). Measurements of  $T_1$  at lower values of  $N$  were not possible because the dot “closed”.

To see what would happen at values of  $N > 1$  in dots that can reach  $N = 0$ , we looked for spin bumps on our InGaAs dot, starting with  $N = 1$ , and progressing all the way up to  $N = 9$ . We found a spin bump at  $N = 1, 3, 5$ , and  $7$ , but none for  $9$ , and none for  $N = 2, 4, 6$ , and  $8$ . These sightings are consistent with Pauli filling of an asymmetric dot [9], in which the spin values would be  $1/2, 0, 1/2, 0 \dots$  for  $N = 1, 2, 3, 4 \dots$  electrons. The measured value of  $T_1$  for  $N = 7$  was 12.8 ms, which is shorter than the 41.5 ms measured for  $N = 1$ , but not dramatically so.

For Si/SiGe dots, however, which have an extra degeneracy due to valleys, there is reason to believe (e. g., see [10]) that the filling sequence for an asymmetric dot should be  $1/2, 1, 1/2, 0, 1/2, 1, 1/2, 0 \dots$  when the Zeeman energy exceeds the valley splitting. For our lowest  $N$ -value, the measured Zeeman splitting and  $g$ -value of 2.0 imply a spin of  $1/2$  (or greater). If the spin is  $1/2$ , the next higher value of  $N$  should have an  $s = 0$  or  $s = 1$  ground state. Measurements of the  $N + 1$  dot showed that the ground state had  $s = 0$ ,

and the excited state  $s = 1$ , with a surprisingly-small singlet-triplet splitting of approximately  $36 \mu\text{eV}$  [11]. Thus we contend that our measured values of  $T_1$  are for an unpaired spin of  $1/2$ , and are representative of (although probably somewhat shorter than) the value that would be obtained for a single-electron spin- $1/2$  dot.

**Theory** At reasonably strong spatial confinement, low temperatures, and small-to-moderate magnetic fields, the single-phonon admixture mechanism dominates the *intrinsic* spin flip ( $T_1$  relaxation process) of zero-dimensional conduction electrons in III-V materials [12]. It can be understood as follows. Spin-orbit (SO) coupling admixes higher orbital states with opposite spin projections into the eigenstates of the lowest spin doublet, thus allowing, in principle, intra-doublet transitions (i. e., spin flip) to be induced by strictly spin-independent interactions with the environment, e. g., with lattice vibrations. Exact cancellation in the transition matrix element, enforced by the time-reversal symmetry of the total electron Hamiltonian (including the SO admixing terms), should be broken by a magnetic field to yield a finite spin relaxation rate.

At low magnetic fields the Zeeman splitting of the SO-mixed doublet (and, thus, the required energy transfer to the lattice phonon) is small, so that, when present, piezoelectric electron-phonon coupling dominates, resulting, at temperatures  $T \ll g\mu_B B/k_B$ , in a well-known [12, 13, 14] functional dependence

$$T_{1P}^{-1} = P\eta^2 B^5/E_0^4$$

obtained in the (valid for our case) approximation of long-wavelength resonant phonons.  $E_0$  is the spatial quantization energy. SO coupling is assumed to be dominated by linear-in- $k$  SO terms in the electron dispersion; their strength is quantified by a material- and structure-specific constant  $\eta$ , which is, in general, anisotropic. In non-piezoelectric materials, but also in piezoelectric materials at larger magnetic fields, energy transfer to phonons is facilitated by a deformation potential coupling resulting (e. g., [14]) in

$$T_{1D}^{-1} = D\eta^2 B^7/E_0^4$$

at low temperatures. At temperatures  $T \gg g\mu_B B/k_B$ , the spin-flip rate is given by  $T_{1P,D}^{-1} k_B T/g\mu_B B$ .

Moderate electric fields  $\lesssim 2 \text{ mV/nm}$  are typically present in our dots. In InGaAs structures, a bulk-inversion-asymmetry-induced (BIA or Dresselhaus) SO term with  $\beta \sim 1600 \mu\text{eV nm}$  dominates the structure-induced (SIA or Rashba) term ( $\lesssim 500 \mu\text{eV nm}$ ), making  $\eta \approx \beta$  a field-independent and *isotropic* constant, so that no in-plane anisotropy is to be expected for  $T_1$  in a circular dot.  $P$  and  $D$  are

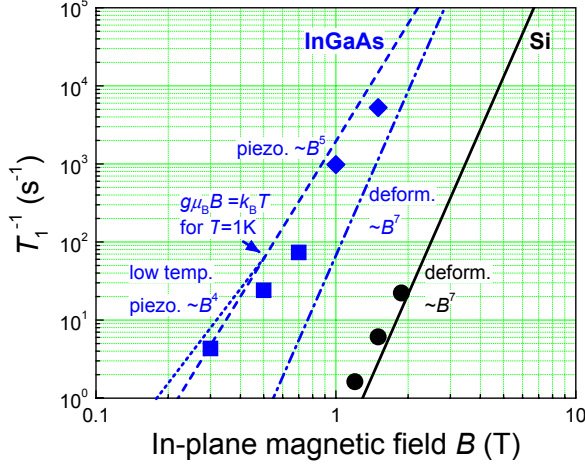


Figure 5: Inverse spin lifetimes as a function of magnetic field. Circles are for the Si depletion dot, squares (diamonds) for the InGaAs depletion (accumulation) dot.  $B$  is always parallel to the 2DEG (along the [010] axis). The straight lines are theoretical predictions for the two material systems.

material-, but not structure-specific parameters (apart from a weak  $g$  factor dependence). When expressing  $T_1^{-1}$  in inverse seconds,  $\eta$  in  $\mu\text{eV nm}$ , the *in-plane*  $B$  in Tesla, and  $E_0$  in meV, the InGaAs-specific constants  $P$  and  $D$  are found to have numeric values of 7.6 and 0.26, respectively [15]. These low-temperature asymptotics of  $T_{1P}^{-1}$  and  $T_{1D}^{-1}$  are shown in Fig. 5 by dashed and dash-dotted lines, respectively, for the relevant  $E_0 = 10$  meV. The dotted line is the high temperature  $B^4$ -asymptote of  $T_{1P}^{-1}$  calculated for  $T = 1$  K. Our measurement temperatures are always much lower.

The Si crystal symmetry allows neither piezoelectricity nor a BIA SO term. SIA is dwarfed by an especially weak bulk SO coupling for  $\Delta$  valleys (estimated to be only 3–4  $\mu\text{eV nm}$  in comparable structures [16]). It was suggested in [17] that linear-in- $k$  SO terms in (001) Si heterostructures are dominated by contributions of a low-symmetry heterointerface. For our typical electric fields, we estimate, with the help of Fig. 3 in [17], that  $\eta$  has a maximum value of 20–30  $\mu\text{eV nm}$  for a perfect interface, but a much lower value in the presence of interface imperfections. In Fig. 5,  $T_{1D}^{-1}$  in Si (with  $D = 4.3 \times 10^{-3}$ ) is shown by solid lines for (the numerically simulated)  $E_0 = 2$  meV.

Other spin-lattice relaxation mechanisms were proposed for Si dots, in particular: (i) the modulation of the hyperfine coupling by phonon deformation, which has a  $B^3$  field dependence [12, 18], and (ii) the phonon-induced modulation of the *bulk* electron  $g$ -factor, with a  $B^5$ -dependence and a strong sensitivity to the orientation of the in-plane magnetic field with respect to the

main crystallographic axes [19]. As formulated, these mechanisms are not directly related to the heterointerface properties. They should exceed  $T_{1D}^{-1}$  at extremely small magnetic fields, but the estimated times are too slow to be observed in our experiments.

**Acknowledgements** We gratefully acknowledge helpful discussions with M.A. Eriksson, H.W. Jiang, and C.M. Marcus. This work was sponsored by the United States Department of Defense. The views and conclusions contained in this document are those of the authors and should not be interpreted as representing the official policies, either expressly or implied, of the United States Department of Defense or the U.S. Government.

\* Electronic address: rrhayes@HRL.com

- [1] M. A. Eriksson *et al.*, Quantum Information Processing **3**, 133 (2004).
- [2] H.-W. Liu *et al.*, Appl. Phys. Lett. **92**, 222104 (2008); H.-W. Liu *et al.*, Phys. Rev. B **77**, 073310 (2008); W. H. Lim *et al.*, Appl. Phys. Lett. **94**, 173502 (2009); A. Fuhrer *et al.*, Nano Lett. **9**, 707 (2009); L. H. Willems van Beveren *et al.*, Appl. Phys. Lett. **93**, 072102 (2008); G. P. Lansbergen *et al.*, Nature Physics **4**, 656 (2008). H. Sellier *et al.*, Appl. Phys. Lett. **90**, 073502 (2007).
- [3] C. B. Simmons *et al.*, Appl. Phys. Lett. **91**, 213103 (2007); M. R. Sakr *et al.*, Appl. Phys. Lett. **87**, 223104 (2005).
- [4] E. Croke, to be published.
- [5] J. M. Elzerman *et al.*, Appl. Phys. Lett. **84**, 4617 (2004).
- [6] J. M. Elzerman *et al.*, Nature **430**, 431 (2004).
- [7] U. Meirav and E. B. Foxman, Semicond. Sci. Tech. **11**, 255 (1995).
- [8] D. K. Wilson and G. Feher, Phys. Rev. **124**, 1068 (1961).
- [9] S. M. Reimann, Rev. Mod. Phys. **74**, 1283 (2002).
- [10] Y. Hada and M. Eto, Phys. Rev. B **68**, 155322 (2003).
- [11] To be published.
- [12] A. V. Khaetskii and Y. V. Nazarov, Phys. Rev. B **64**, 125316 (2001).
- [13] L. M. Woods *et al.*, Phys. Rev. B **66**, 161318 (2002).
- [14] P. Stano and J. Fabian, Phys. Rev. Lett. **96**, 186602 (2006); Phys. Rev. B **74**, 045320 (2006).
- [15] Derived using InGaAs- and Si-specific data in *Intrinsic Properties of Group IV Elements and III-V, II-VI, and I-VII Compounds*, edited by O. Madelung, Landolt-Boörnstein, New Series, Group III, Vol. 22, Pt. A (Springer, Berlin, 1987) and *Semiconductors — Basic Data*, edited by O. Madelung (Springer, Berlin, 1996); an isotropic elastic continuum is assumed;  $g_{\text{in-plane}} = -3.5$  is calculated for our biased InGaAs structure and agrees well with the experiment.
- [16] Z. Wilamowski *et al.*, Phys. Rev. B **66**, 195315 (2002); C. Tahan and R. Joynt, Phys. Rev. B **71**, 075315 (2005).

- [17] M. O. Nestoklon *et al.*, Phys. Rev. B **77**, 155328 (2008).
- [18] A. V. Khaetskii, Photonics Spectra **10**, 27 (2001).
- [19] B. A. Glavin and K. W. Kim, Phys. Rev. B **68**, 045308 (2003).